Experimental Study of Kinetic Processes During the Steel Treatment at two LMF's

Jörg Peter
Kent D. Peaslee
David G. C. Robertson

University of Missouri-Rolla
Department of Materials Science and Engineering
1870 Miner Circle
218 McNutt Hall
Rolla, MO 65409-0340
Tel.: 573-341-4714
Fax: 573-341-6934
E-mail: jjpeter@umr.edu or kpeaslee@umr.edu

Brian G. Thomas

University of Illinois at Urbana-Champaign
Mechanical and Industrial Engineering Department
1206 West Green Street
Urbana, IL 61801
Tel.: 217-333-6919
Fax: 217-244-6534

Keywords: ladle refining, mass transfer rate constant, kinetics, industrial trials

ABSTRACT

The mass transfer rate during ladle refining was quantified by taking sequential steel and slag samples during the treatment of 20 heats. Each heat was stirred with a different argon flow rate, ranging between 0 and 63 scfm. Heats were treated at two different plants. Al-killed steel was produced at an LMF in 151-t ladles. Si-deoxidized steel was produced at an LMF in 123-t ladles. Mass transfer rate constants were determined for each heat by using process simulation (Metsim) and thermodynamic (FactSage) models. Relationships between mass transfer rate constants and stirring powers as well as ladle geometries were compared between the two plants and published literature. It was found that the reaction kinetics during ladle refining depend on the bulk transport of the steel to the slag/steel interface and on the thermodynamic equilibrium at the slag/steel interface. The necessary refining time decreases if the newly-defined specific steel transport rate is maximized and the slag has a low basicity and FeO concentration before the start of de-S.

INTRODUCTION

Ladle Metallurgical Furnaces (LMF's) are used for steel temperature control, deoxidation of the steel, reduction of sulfur, alloy additions, inclusion floatation and modification, as well as a holding unit if delays occur during production. Reaction rates that lead to the desired steel composition within short times are desired in order to increase production or to avoid delays. The steel is stirred to homogenize the steel and to transport the steel to the slag/steel interface were most reactions occur. Industrial trials were performed at two different LMF stations to gather information about the correlation of the argon flow rate, reaction rates, and thermodynamic factors that could influence the necessary treatment time of the steel at these LMF's. The results of this study will also be used to design and simulate a new, fully continuous steelmaking process.

EXPERIMENTAL PROCEEDURE

The treatments of 20 heats at two different LMF's were observed at different argon flow rates. The monitored heats included 12 heats with Al-killed steel at LMF 1, using argon flow rates between 50 and 63 scfm and 8 heats with Si-deoxidized steel at LMF 2, using argon flow rates between 0 and 15 scfm. The experiments were a detailed time study of ladle additions, stirring conditions, and the resulting steel and slag compositions and steel temperatures. The recorded details of the ladle treatment included amount, time, and type of alloys and fluxes, temperature measurements, dissolved O measurements, start and end of arcing, start and end of argon stirring with corresponding flow rates and pressures, estimated steel masses, estimated amount of solid and liquid slag, as well as miscellaneous information such as the falling of a scull from the roof into the steel. A video camera was used to record times of additions, samples, and temperature measurements with a precision of one second.

The change of the composition of the steel and slag was measured by taking between 25 to 30 steel samples as well as 3 to 6 slag samples while the steel was treated at the LMF. The treatment durations ranged between 25 and 45 minutes. Steel samples were taken every 30 to 90 seconds and slag samples were taken every 5 to 10 minutes. A time was assigned to each sample based on video tapes that were recorded during treatment of each heat. Immediately after the steel samples were taken, they were dropped into labeled steel cans that were filled with water and held by a wooden box. The steel samples were placed into labeled envelops after they cooled. The chemistries of the steel samples were analyzed with a mass spectrometer. A LECO machine was used to determine the nitrogen and total oxygen of each steel sample.

The slag samples were taken with a pole at LMF 1 and with a spoon at LMF 2 and placed in sequential order on the ground. The cooled slag samples were placed into labeled envelops. The slag samples from LMF 1 were analyzed with an X-ray fluorescence (XRF) machine. The slag samples from LMF 2 were analyzed by ACME Analytical Laboratories using Induction Coupled Plasma Emission Spectrometer (ICP-ES) for determining the concentrations of all oxides except FeO, dichromate titration for determining the FeO, a LECO machine for determining the sulfur, and ion electrode analysis for determining the fluorine content of the slag. In addition, 9 slag samples from LMF 2 that contained little CaF_2 were analyzed by XRF, as well. The double analysis allowed for a comparison of the results, which agreed well. A magnet was passed over the grinded and spread-out slag powders before the analysis to remove metallic iron.

DISCRPTION OF METSIM MODEL

Metsim is a program capable of performing dynamic simulations of a multitude of processes. A model was designed to simulate the 20 heats. The model uses data from the industrial trials as inputs, including the initial compositions and estimated masses of the steel and slag; time, type, and amount of additions, and temperatures. The estimated initial slag mass was often corrected within the simulations so that flux and reaction product additions agreed with the recorded concentration changes of slag components. The outputs of the Metsim program are calculated steel and slag concentrations with associated times. This output was graphed together with the concentration and time data from the industrial trials. The mass transfer rate constant was adjusted within the Metsim model until the calculated concentrations agreed with the measured data for all components of the steel and slag. In this way, the simulations were used to determine 26 different mass transfer rate constants for 26 different argon flow rates. These mass transfer rate constants not only reflect the concentration change of one steel component (e.g. S) but the concentration changes of all components of the steel and slag.

The mass transfer rate constant

The value of the mass transfer rate constant (k) represents the fraction of the steel that reacts with the slag during one minute. It has the unit of inverse minute (min^{-1}). Equation 1a shows a first-order rate equation with the mass transfer rate constant. The solution of Equation 1a is Equation 1b, which is an exponential function that describes the decrease of concentration (C) over time (t), starting with an initial concentration (C_o). The equilibrium concentration (C_{equ}) is assumed constant in Equation 1.

Equation 1a $$\frac{dC}{dt} = -k\left(C - C_{equ}\right)$$

Equation 1b $$C = C_{equ} + \left(C_o - C_{equ}\right)e^{-kt}$$

The Metsim model for steel treatment in ladles

Process models may be built with a multitude of modules and streams within Metsim. The modules called Free Energy Minimizer (FEM's), mixer, splitter, and streams were used to create a model of a ladle. Streams allow for material flow among the modules, using metric tons per hour (mt/hr) as a unit.

The ladle model is illustrated in Figure 1. The slag/steel reactions were calculated with the Interface FEM and the reaction within the steel were calculated with the Bulk FEM. The temperature for the calculations in these FEM's was set to be the measured temperature from the trials. The pressure was set at 1.3 atm in the Bulk FEM and at 1 atm in the Interface FEM. Activity coefficients (γ) of elements and compounds were chosen based on FactSage calculations so that the Metsim FEM's produced similar results than the FactSage FEM for the range of the measured steel and slag chemistries. This procedure required numerous iterations of the Metsim simulations and the change of some activity coefficients during the calculations. For instance, the activity coefficient of liquid FeO had to be adjusted during and after deoxidation of the steel. The values of the FeO activity coefficients ranged between 0.9 and 3.2.

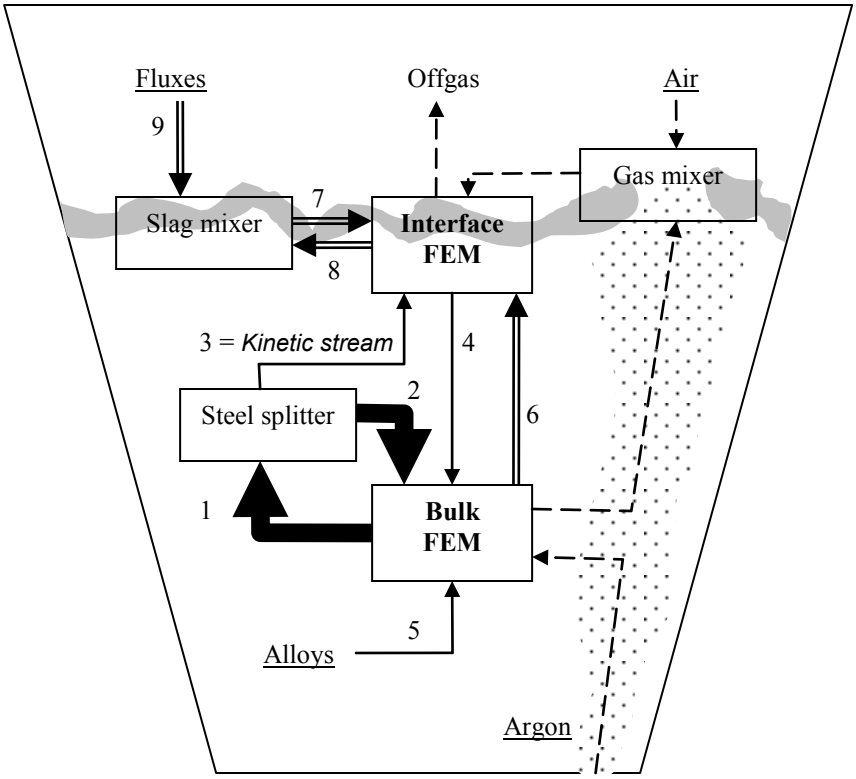

Figure 1: Illustration of Metsim model used for simulation of steel treatment in the ladle

The wide, solid streams (1, 2) in Figure 1 represent the bulk flow of the steel that does not react with the slag during one calculation. The width of these streams indicates that the majority of the steel does not react with the slag during each calculation. The time step for each calculation was chosen to be ten seconds. The flow of stream 1 is the quotient of the total steel mass and the time step. The flow of the returning stream 2 is the difference between stream 1 and the flow of the *Kinetic Stream* 3. The flow of the *Kinetic Stream* 3 is the product of the total steel mass and the mass transfer rate constant (k). This flow was adjusted until the simulation results agreed with the data from the industrial trials. Stream 4 represents the steel flow from the slag/steel interface back into the bulk. Alloys with compositions as provided by the suppliers were added through stream 5 at times that were recorded during the industrial trials.

Streams that carried oxides or other non-metallic liquids are represented by double lines. Stream 6 transported inclusions from the Bulk FEM to the Interface FEM. Stream 7 and 8 carried slag between the Interface FEM and the Slag mixer, representing a well mixed slag. Fluxes with compositions as provided by the suppliers were added with stream 9 at times that were recorded during the industrial trials. Dashed lines in Figure 1 illustrate gas streams. Argon entered the Bulk FEM at the recorded flow rates. The product gases from the Bulk FEM mixed with air and than reacted with the steel and slag in the Interface FEM. The air intake was adjusted so that the model predicted the measured nitrogen increase. Off-gases left the system from the interface FEM.

Mass transfer within the slag

The rate of the reactions on the slag/steel interface depends on the mass transport of all reactants to the interface and the mass transport of all products away from the interface. Reactions rates are increased if species are frequently transported to and away from the interface and if the interface is large.

Argon stirring is usually chosen as the preferred stirring method for refining (over induction stirring) because it not only transports the species to and away from the slag/steel interface but it also creates a large slag/steel interface or emulsion in the upper part of the

ladle. Lachmund et al.[1] recorded in detail the number, sizes, and size distribution of slag droplets within the steel in the upper part of an industrial ladle, documenting large slag/steel emulsion during argon stirring. Grip and Jonnson[2] measured slag compositions at different locations and could not find a significant difference between their measurements, drawing the conclusion that the slag is well mixed. In addition, Grip and Jonnson[2] recorded that the steel splashes on top of the slag, creating slag/steel emulsions. Vigorous mixing of the slag with the steel was also observed during the treatment of all 20 heats that are evaluated in this report. For instance, numerous slag particles were observed in the steel samples even at argon flow rates as low as 2 scfm. These observations and results agree with the findings of El-Kaddah and Szekely[3] who concluded that the limiting factors for reaction kinetics within argon-stirred ladles are the bulk transport of the steel to slag/steel interface and the thermodynamic equilibrium at the slag/steel interface but not the emulsion or interfacial area.

An early version of the Metsim ladle model included a slag splitter, allowing for the calculation of the mass transfer rate constant on the slag side of the slag/steel interface. The results of this more complex model were compared to the results of the simpler model that is shown in Figure 1, finding no significant differences between the two models. This result can not only be explained with a well-mixed, low-volume slag, and with the ease of creating slag/metal emulsions but also with the relationship among the different mass transfer rate constants. Equation 2 describes the relationship between the overall mass transfer rate constant (k), the mass transfer rate constant for the slag (k_S), and the mass transfer rate constant for the steel (k_M).

Equation 2:
$$\frac{1}{k} = \frac{1}{k_S L} + \frac{1}{k_M}$$

The distribution ratio (L) of a species (e.g. S) is the ratio of the concentration of this species on the slag/steel interface in the slag and the concentration of the species on the slag/steel interface in the steel. The distribution ratios range between 100 and 700 for sulfur, making the first summand of Equation 2 significant smaller than the second summand for slags that are at least as well stirred as the steel. As a result, the overall mass transfer rate constant is determined by the mass transfer rate within the steel ($k \approx k_M$).

DISCUSSION OF DATA AND SIMULATION RESULTS

General information

The chemical analysis of approximately 600 steel samples and 100 slag samples were compared with the Metsim simulations, using 80 graphs. It is not feasible to report all the data and simulation results in this paper. However, the data was summarized and one representative heat from each LMF was chosen for illustration of all data and simulation results.

The estimated steel and slag masses, recorded lime additions, and average temperatures together with ladle dimensions (fill height, average and top inner diameters) and numbers of porous plugs for each LMF are summarized in Table 1. Flux additions during or after the deoxidation of the steel included lime for all heats as well as 250 lbs to 750 lbs of bauxite during the treatment of heats 1 to 6 (LMF 1) and 375 lbs of spar and 40 lbs to 80 lbs of MgO during the treatment of all heats from LMF 2 (heats 13 to 20). The slag masses in Table 1 are based on the initial estimate and the corrections of these estimates that were made during the simulations. The initial slag is the slag after the Al-kill for LMF 1 and before the Si-deoxidation for LMF 2.

Table 1: General information from each LMF (averages)

	Steel	Initial slag	Final slag	Lime	Temp.	Fill height	Ladle D_{avg}	Ladle D_{top}	plugs
	tons	tons	tons	tons	ºF	inches	inches	inches	number
LMF 1	151	2.0	3.3	1.2	2932	119	115	118	2
LMF 2	123	1.6	3.0	1.0	2837	121	103	108	1

Two representative heats

The change of steel and slag composition during the treatment of two heats over 30 minutes is shown in Figure 2. The data and simulation results from heat 8 (LMF 1) are shown in the left column of Figure 2 (Figure 2a); and the data and simulation results from heat 16 (LMF 2) are shown in the right column of Figure 2 (Figure 2b). The measured data is presented as discrete data points whereas the results from the simulations are presented as continuous lines. The simulations could reproduce the measured steel and slag concentrations during all times and for all heats.

The concentrations of C, P, S, Si, and Al in the steel are reported in the first row of Figure 2 followed by the concentrations of Mn, V, N, and total O in the second row. The concentration of nitrogen was multiplied by 100 in order to present several elements in one graph. The graphs in the last two rows show the composition of the slags, reporting CaO, SiO_2, Al_2O_3, P, and S in the third row and MgO, MnO, and CaF_2 in the final row of Figure 2. Heat 8 was stirred with 50 scfm with a corresponding mass transfer rate constant of 0.18 min^{-1}; and heat 16 was stirred with 7 scfm with a corresponding mass transfer rate constant of 0.06 min^{-1}.

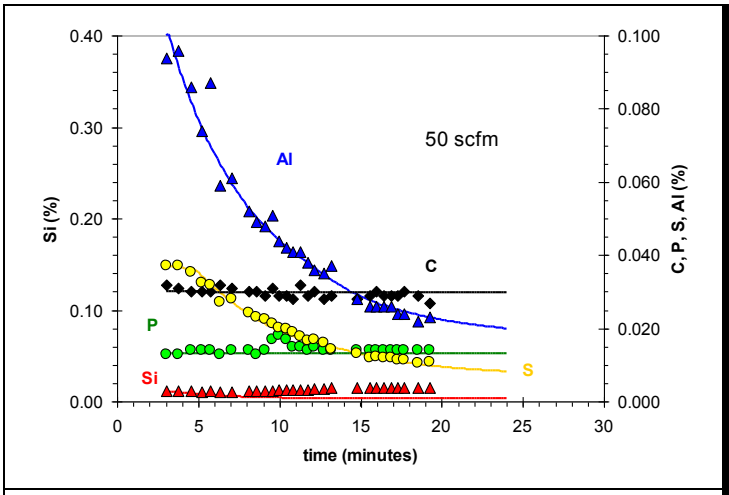

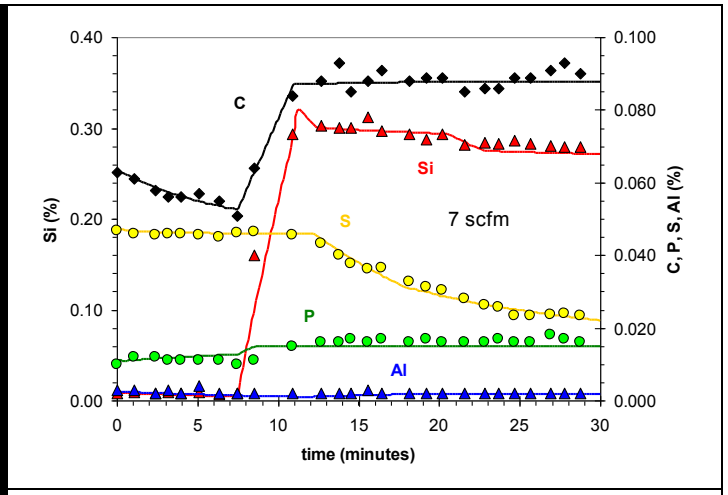

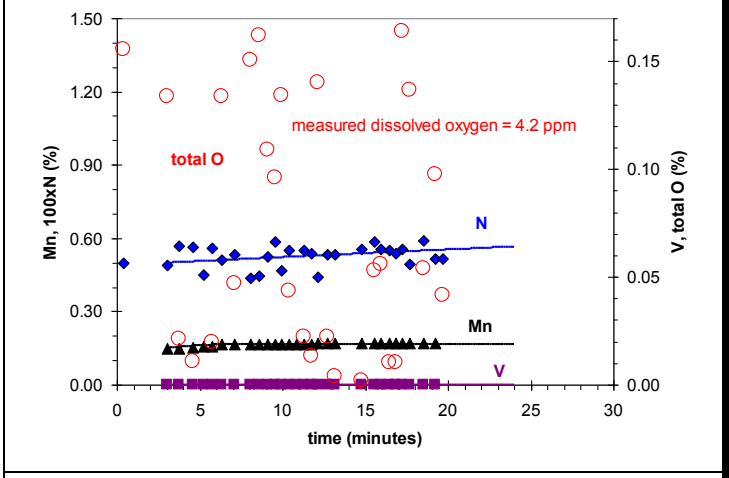

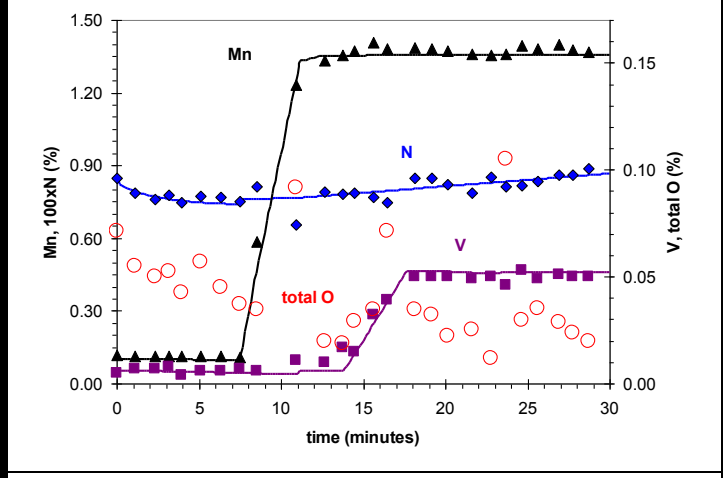

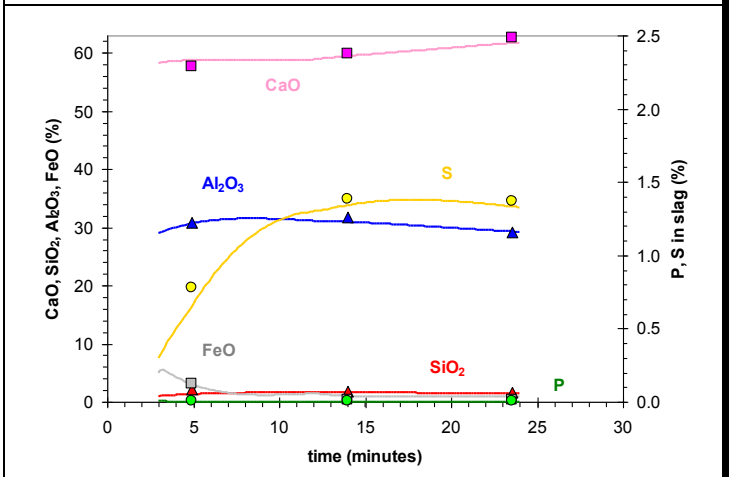

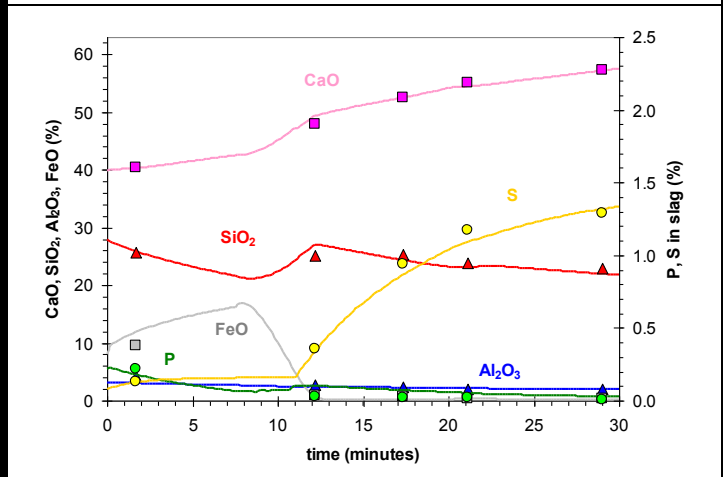

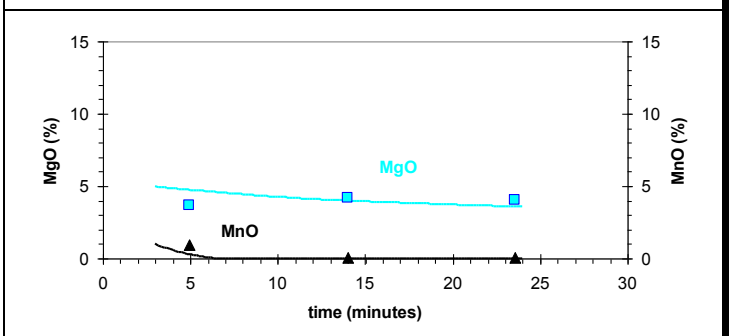

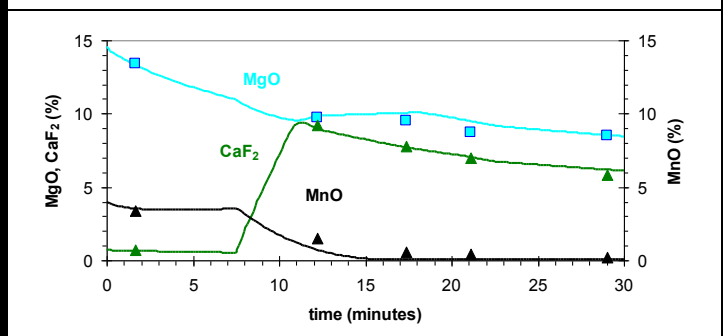

Figure 2a: Data and simulation results from heat 8 (**LMF 1**)

Figure 2b: Data and simulation results from heat 16 (**LMF 2**)

Al-killed steel was produced with heat 8. Aluminum was added during the first 3 minutes of the treatment. Lime was added after the first minute (1000 lbs), after the eight minute (785 lbs), and after the 15th minute (800 lbs), increasing the basicity of the slag and aiding desulfurization (de-S). 500 ft of Al-wire was added after the last steel sample was taken shortly before the ladle left the LMF. Al decreased from 0.094% to 0.023% and S decreased from 0.037% to 0.011% while steel samples were taken. The Al_2O_3 content in the slag slightly decreased during the treatment because lime was added. This decrease reduced the activity of Al_2O_3, supporting a speedy de-S. The rate of de-S was also enhanced by the decrease of the FeO content from 5% to 1% during the first 5 minutes after the kill. A total of 350 lbs of iron oxide (Fe_2O_3) had to be added during the simulated time in order to reproduce the decrease of the aluminum concentration. The sulfur content of the slag increased from 0.3% to 1.4%.

The concentration of carbon and phosphorus did not change while samples were taken. Their concentrations were 0.030% and 0.014% respectively. Alloys were not added to the steel during the treatment of this heat. The manganese increased slightly due to the reduction of MnO during and after the kill. The Si concentration increased from 0.012% to 0.015% during the treatment, indicating the reduction of SiO_2 from the slag. However, the simulation could not predict the Si-reversion.

The nitrogen increased from 50 ppm to 55 ppm over a period of 20 minutes due to open eye where the steel is exposed to the air. The steel was not heated with the electrodes during the entire treatment since the temperature of the steel was 3010ºF at the end of the kill and 2936ºF after 19 minutes. The total oxygen varied between 22 ppm and 1700 ppm during the entire treatment time, while the dissolved oxygen was measured to be 4.2 ppm. The "shut-gun" pattern of the total oxygen indicates that plenty of slag is entrapped in the steel, qualitatively reproducing the results from Lachmund et al[1].

The total oxygen varied between 120 ppm and 1050 ppm during the treatment of heat 16 while Si-deoxidized steel was produced. These results agree with previous measurements on LMF 2 by Mannering[4]. The lower maximum total oxygen (as compared to heat 8) could be an indication that the slag/steel emulsion is less at lower argon flow rates. However, the nitrogen increase during steel treatment does not seem to be a function of argon flow rate, the size of the open eye, nor the duration of arcing. The nitrogen increased at the same average rate (0.25 ppm / min) during heat 16 as during heat 8. The nitrogen increased from 80 ppm before the seventh minute to 86 ppm after 30th minute. Heat 16 was periodically arced, maintaining an average steel temperature of 2850ºF.

The nitrogen slightly decreased from 84 ppm to 80 ppm during the first seven minutes of the treatment of heat 16 due to a carbon boil. The carbon decreased from 0.063% to 0.051% during the boil. The only steel treatment during this time was argon stirring and the addition of 120 lbs of lime. The simulation predicted that the FeO content of the slag increased from 8% to 16% during these seven minutes. A FeO concentration of 9.5% was measured after the second minute. Prolonged argon stirring before the addition of deoxidants and alloys is usually not practiced. It was done during the trials to test the amount of carbon that could be removed with such a practice within a reasonable time.

The FeO concentration of the slag decreased within four minutes to a value of 0.9% while 4682 lbs of SiMn, 264 lbs of FeSi, 375 lbs of spar, and 500 lbs of lime were added. The low FeO concentration was necessary for de-S to start around the 12th minute. The phosphorus increase (0.002%) during alloy additions originated to 80% from the SiMn that contained 0.45% P while the rest of the phosphorus increase was due to the reversion from the slag. The carbon content of the steel increased from 0.051% to 0.088% during the alloy addition because the SiMn contained 1.9% C. The SiO_2 content of the slag increased during deoxidation of the steel while the MnO concentration decreased. The SiO_2 concentration decreased after deoxidation due to continuous lime additions, decreasing the activity of SiO_2 and supporting a speedy de-S. The CaF_2 content of the slag increased to 9.3% during the alloy additions and decreased afterwards to a final value of 6.0% due to continuous lime additions and due to evaporations. The CaF_2 concentration of 0.7% before the addition of spar indicates that approximately half a ton of the slag from the previous heat was left in the ladle.

Vanadium (100 lbs) and MgO (40 lbs) were added after the 14th minute, increasing the vanadium concentration to its final value of 0.051%. Part of the scull from the LMF roof fell into steel around the 20th minute, supplying iron oxide to the system. At this time, 230 lbs of Fe_2O_3 had to be added to the model to reproduce the measured concentrations. The supply of iron oxide caused a decrease of the silicon concentration in the steel and a slowing of the de-S rate, in spite that 78 ft of CaSi wire was added two minutes after the oxidized scull fell into the steel.

The correlation between the mass transfer rate constant and the specific stirring power

The mass transfer rate constants of all 20 heats together with the corresponding argon flow rates and specific stirring powers are listed in Table 2. Previous researchers[1, 5, 6] compared the mass transfer rate constant to the specific stirring power (ε). The specific stirring power is a function of the argon flow rate at standard temperature and pressure (Q), the steel mass (m), the injection depth of the argon (h), the ambient pressure above the bath (P_o), and the absolute steel temperature (T). Metric units are required when the stirring power formula is used as it is written in Equation 3. The specific stirring power has the unit watts per metric ton (W/mt). Lehner[7] published a derivation of the stirring power formula, accounting for the buoyancy work and pressure-volume work that is transferred to the steel during the rise of gas bubbles. The stirring power formula assumes that each steel particle receives the same, average amount of kinetic energy during the time of argon stirring.

Equation 3:

$$\varepsilon = 14.23 \frac{QT}{m} log_{10}\left(1 + \frac{h}{1.5P_o}\right)$$

Table 2: Measured argon flow rates at STP, calculated specific stirring powers, and calculated mass transfer rate constants

LMF 1													
Heat number		1	2	3	4	5	6	7	8	9	10	11	12
Ar	scfm	60	61	63	63	63	52	61	50	56	61	55	62
ε	W/mt	159	160	165	165	171	136	159	135	148	162	146	164
k	min^{-1}	0.19	0.18	0.18	0.20	0.20	0.17	0.17	0.18	0.20	0.20	0.16	0.21

LMF 2															
Heat number		13			14	15	16	17			18			19	20
Ar	scfm	2	4	6	15	4.5	7	10	0	4	13	0	4	13	8
ε	W/mt	6	13	19	47	14	23	32	0	13	42	0	13	42	26
k	min^{-1}	0.05	0.05	0.11	0.12	0.08	0.06	0.10	0	0.06	0.12	0	0.07	0.10	0.08

The specific stirring power is mainly a function of the argon flow rate and steel mass for the production conditions that are practiced at both LMF's because the ambient pressure was always one atmosphere, because the absolute temperature varied little, and because the argon was injected at the bottom of all ladles that were filled approximately 10 feet high with steel. The relationship of the mass transfer rate constant to the specific stirring power is shown in Figure 3 for 26 different argon flow rates that were used during the treatment of 20 heats.

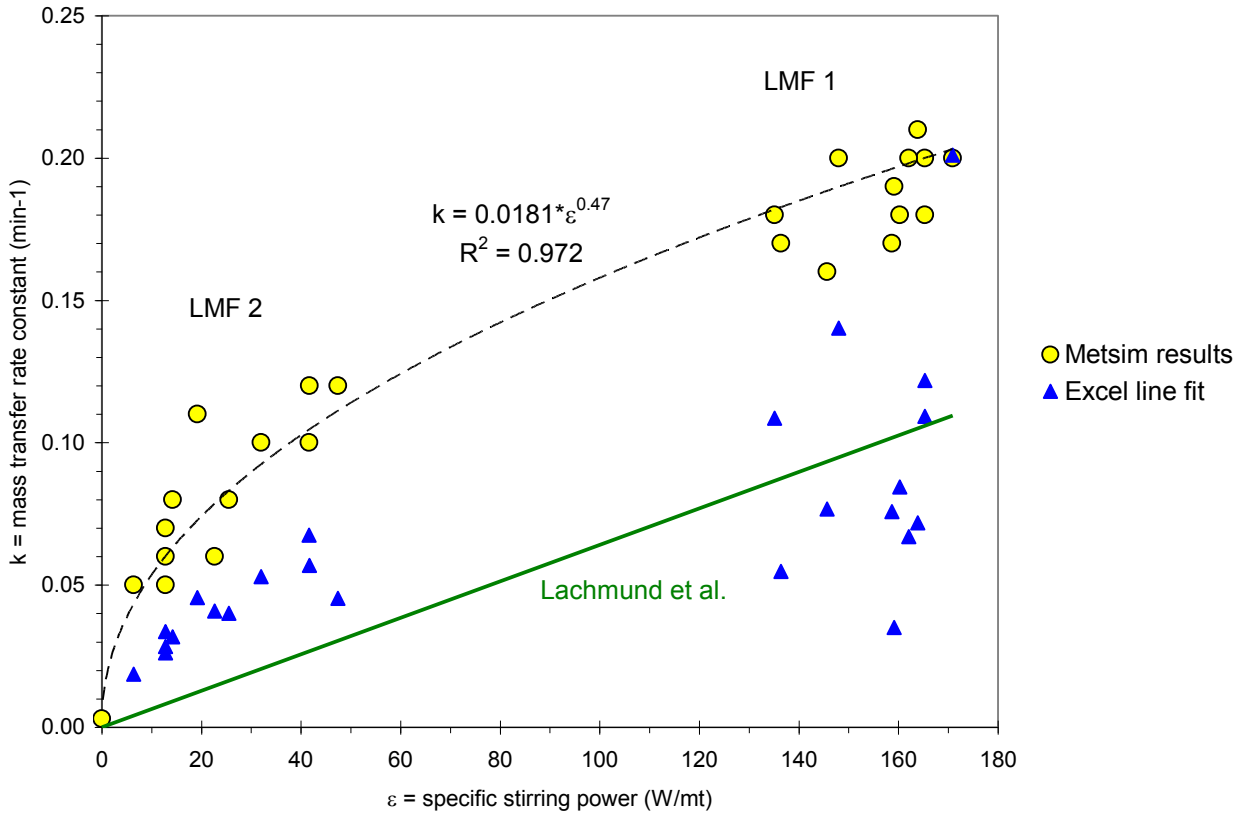

Figure 3: Relationship between mass transfer rate constant and the specific stirring power

The circles in Figure 3 represent the values of the mass transfer rate constants that were calculated with Metsim. A power function with an exponent of 0.47 fit the relationship between the mass transfer rate constant and the specific stirring power (R^2 = 0.97). This relationship was expressed with similar power functions by previous researchers. Ghosh[5] and Qu[6] published summaries of the results from previous works. The reported exponents for industrial reactors range between 0.27 and 1.0 with an average of 0.54.

The triangles in Figure 3 represent the exponent of Equation 1b that were calculated by fitting an exponential function to the recorded times and the differences between the measured sulfur concentrations and the final equilibrium sulfur concentration. The final equilibrium sulfur concentrations were calculated with FactSage and ranged between 3 ppm and 41 ppm for both types of steels. Equation 1b assumes that the equilibrium sulfur concentration at the slag/steel interface is constant and at its final value during the entire refining time. This assumption is incorrect because simulation results show that the equilibrium sulfur concentration at the steel/slag interface at the start of de-S is up to 50% of the initial bulk sulfur concentration, depending on the activity of the FeO in the slag at this time and the choice of deoxidant (Al or Si). If the assumption of a constant, low value of the equilibrium sulfur concentration would be correct, there would be only a weak correlation between the mass transfer rate constant and the specific stirring power because the values that were calculated with this assumption (triangles) do not show a clear relationship in Figure 3 (R^2 = 0.49 for linear fit), especially for data from LMF 1 (Al-killed steel).

The solid line in Figure 3 represents the correlation between the mass transfer rate constant and the specific stirring power as published by Lachmund et al[1]. Their data is comprehensive and most recent; however, it does not agree with the results of this work. Instead, the results from Lachmund et al. seem to fit more closely the values that were calculated with a line fit.

ADDITIONAL EVALUATIONS OF THE DATA AND SIMULATION RESULTS

The current work could approximately reproduce the average of the published exponents (~0.5) for the power function that describes the relationship between the mass transfer rate constant and stirring power. These results point to a square-root relationship between the mass transfer rate constant and the stirring power.

On the other hand, the stirring power formula incorrectly assumes an equal power input to all parts of the ladle. Aoki et al[8] published fluid flow models of argon-stirred ladles that were verified with measurements from LMF 2, documenting different flow regimes throughout the ladle. The largest velocities, turbulences, and energy dissipation rates occurred within the plume and in the vicinity of the slag/metal interface just as predicted by El-Kaddah and Szekely[3]. Another incongruity of the stirring power formula is the absence of an area term in the numerator, implying that the ideal shape of a steel refining vessel is a tall, thin tube. A dimensional analysis was performed to increase the understanding of relationship between common production conditions and the mass transfer rate constant.

Dimensional Analysis

The mass transfer of the steel from the bulk to the slag/steel interface depends on the energy input (Q), the fluid flow within the steel, which is a function of the shape and size of the vessel (h, H, D_{avg}, D_{top}), and variables that are important for emulsification (ρ_M, ρ_S, μ_M, μ_S, σ, H_S). The 13 variables that were considered during the dimensional analysis (Table 3) have three basic dimensions (length, time, and mass), requiring ten dimensional groups (Table 4).

Table 3: List of 13 variables that were considered in the dimensional analysis

Symbol	Name of variable	Symbol	Name of variable	Symbol	Name of variable
k	mass transfer rate constant	g	gravitational constant	μ_M	steel viscosity
Q	argon flow rate	H_S	height of slag layer	μ_S	slag viscosity
H	fill height	h	injection depth of argon	σ	surface tension
D_{avg}	average diameter	ρ_M	steel density		
D_{top}	top diameter	ρ_S	slag density		

The first two of the ten dimensional groups of Table 4 were used to formulate Equation 4. The other eight groups of Table 4 were not included in Equation 4 because it is assumed that the emulsification is not a limiting factor for the reaction rate and because the values of the last three groups do not significantly vary between the two LMF's. Furthermore, steel and slag masses were included in the Metsim simulation that calculated the mass transfer rate constant and therefore do not need to be included in Equation 4. The derivation of Equation 4 included the change of the squared-top-diameter term (D^2_{top}) to top area (A_{top}) and the change of the cylindrical-volume term (HD^2_{avg}) to steel mass (m).

Equation 4:
$$k \propto \frac{\sqrt{QA_{top}\sqrt{gh}}}{m}$$

Table 4: Ten dimensionless groups from the dimensional analysis

Dimensionless group	Description of group	Reasons for use in Equation 4
$\frac{k^2 HD_{avg}^2}{gD_{top}^2}$	$\frac{mass\,transfer}{interfacial\,area}$	It **was used** because it describes the fraction of steel volume that is transported to a specific slag/steel interfacial area.
$\frac{Q}{HD_{avg}^2}\sqrt{\frac{h}{g}}$	Froude number = $\frac{\text{inertia}}{\text{gravity}}$	It **was used** because it describes the amount of argon flow rate per steel volume and it considers the injection depth.
$\frac{\rho_M^2 gHD_{avg}^2}{\mu_M^2}$	Grashof number = $\frac{\text{gravity}}{\text{vis cos ity}}$	These four groups describe properties that are important for emulsification. The groups were <u>not used</u> because viscosities, densities, and surface tensions were not measured and because it is assumed that emulsification is not the limiting factor for reaction rates in industrial ladles.
$\frac{\rho_M gD_{avg}^2}{\sigma}$	Bond number = $\frac{\text{gravity}}{\text{surface\_tension}}$	
$\frac{\mu_S}{\mu_M}$	Ratio of the slag and steel viscosities.	
$\frac{\rho_S}{\rho_M}$	Ratio of the slag and steel densities.	
$\frac{H_S}{H}$	This ratio is effectively the ratio of the slag and steel masses.	It was <u>not used</u> because the masses of both liquids are incorporated in the Metsim simulations.
$\frac{h}{H}$	Ratio of injection depth and fill height	It was <u>not used</u> because it is 1.0 for both LMF's.
$\frac{H}{D_{avg}}$	Ratio of the fill height and the average diameter.	It was <u>not used</u> because it is similar between the two LMF's (1.03 fro LMF 1 and 1.17 for LMF 2).
$\frac{D_{top}}{D_{avg}}$	Ratio of the top and average diameters.	It was <u>not used</u> because it is similar between the two LMF's (1.03 fro LMF 1 and 1.05 for LMF 2).

Equation 4 was changed to Equation 5a because the algebraic velocity term ($\sqrt{gh}$) in Equation 4 implies constant forces. However, the magnitudes of the buoyancy and pressure-volume forces change while argon bubbles rise through the steel and these forces are a function of the ambient pressure. These forces are correctly described by the stirring power formula, using absolute temperature and the logarithmic term, which is derived by integration[7]. In addition, the effect of the cross-sectional area of the gas inlet or the number of porous plugs ($N^{1/4}$) was included in Equation 5a based on results from a similar dimensional analysis that was published by Zlokarnik[9]. A proportionality constant (C) was included in Equation 5a as well.

Equation 5a:
$$k = \frac{C}{m}\sqrt{14.23\frac{QTA_{top}}{N^{1/4}}\log_{10}\left(1+\frac{h}{1.5P_o}\right)}$$

Equation 5b:
$$\text{unit of } \tau = \frac{\sqrt{N\frac{m^3}{s}}}{mt}$$

The right hand term of Equation 5a was named "specific steel transport rate" (τ) because it includes the argon flow rate as well as the change of momentum that the argon flow rate can transfer to the steel to make it flow (transport). The force that is transferred to the steel by a specific argon flow rate increases if the steel mass is minimized and if the top area and injection depth are maximized. The unit of the specific steel transport rate (Equation 5b) includes the change of momentum of the steel in Newtons (N), the argon flow rate in cubic meters per second (m^3/s), and the steel mass in metric tons (mt). Equation 5a predicts a square-root relationship between the mass transfer rate constant and the argon flow rate and it implies that the shape of an ideal refining vessel is a cone.

A cone-shaped reactor would minimize the amount of steel that needs to be transported by the argon flow while maintaining a sufficient top area to maximize slag/metal reactions and a sufficient fill height to maximize the power input from the argon flow. It maximizes the fraction of the steel that is highly stirred because the largest velocities, turbulences, and energy dissipation rates occur within the plume and in the vicinity of the slag/metal interface, which make up a larger fractional volume of a cone as compared to a cylinder. The fluid flow within an argon-stirred, cone-shaped steel refining vessel was modeled by Zhang et al. (**?!?!?**)

Specific steel transport rate

The result of the dimensional analysis (Equation 5a) was assessed. The specific steel transport rates of the 20 heats and 26 argon flow rates are plotted against the Metsim-calculated mass transfer rate constants in Figure 4. The relationship between these two variables is Equation 5c ($R^2 = 0.96$), which requires metric units and the argon flow rate at STP. The y-intercept of Equation 5c is zero, indicating that the parameters that influence emulsification do not affect the mass transfer rate constant for the production conditions of these two LMF's. This conclusion agrees with the calculations from El-Kaddah and Szekely[3].

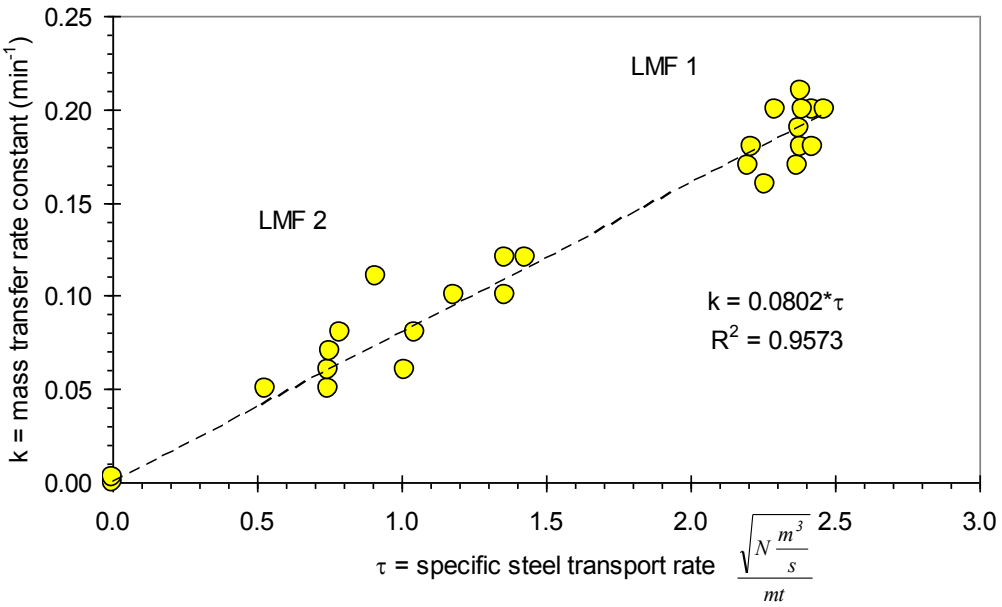

Figure 4: Relationship between the mass transfer rate constant as calculated with Metsim and the specific steel transport rate

Equation 5c:
$$k = \frac{0.08}{m}\sqrt{14.23\frac{QTA_{top}}{N^{1/4}}\log_{10}\left(1+\frac{h}{1.5P_o}\right)}$$

Thermodynamic factors that affect reaction rates

Large reaction rates not only require a frequent transport of steel to slag/steel interface (e.g. large τ) but also thermodynamical conditions at the slag/steel interface that favor desired reactions (e.g. de-S). The thermodynamic equilibrium on the slag/steel interface was different for each heat, causing different de-S rates for similarly stirred heats.

The rate of de-S and the change of Al, Al_2O_3, and FeO concentrations during the treatment of heat 1 and 5 are shown in Figure 5 from the time de-S started until the end of the ladle treatment at LMF 1. The mass transfer rate constant was 0.19 min^{-1} during the treatment of heat 1 and 0.20 min^{-1} during the treatment of heat 5. The bulk sulfur and aluminum concentrations decreased linearly at a rate of 0.001 %S per minute and 0.002 %Al per minute during steel refining of heat 1; whereas these concentrations decreased exponentially at an average rate of 0.003 %S per minute and 0.005 %Al per minute during the treatment of heat 5. The FeO content before de-S was 12.4% in the slag of heat 1 and 3.2% in the slag of heat 5. The Al_2O_3 content of the slag from heat 1 increased from 19% to 34% during the first twelve minutes of de-S and the Al_2O_3 content of the slag from heat 5 was approximately 35% during the entire time of de-S. The basicity (B) of the liquid slag before de-S was 3.3 for heat 1 and 2.4 for heat 5. The basicity (B) was calculated with Equation 6, using the weight percent of liquid slag components based on measured slag concentrations and FactSage calculations.

Equation 6:
$$B = \frac{CaO + 1.4MgO}{SiO_2 + 0.6Al_2O_3}$$

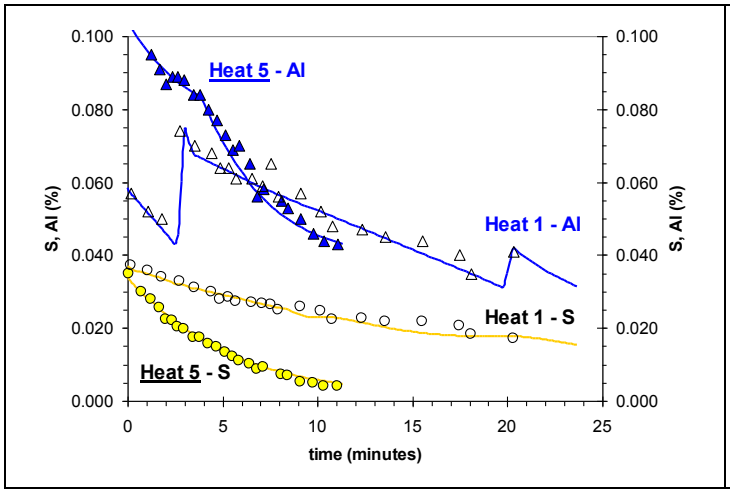

Figure 5a: S and Al concentrations of heat 1 and 5

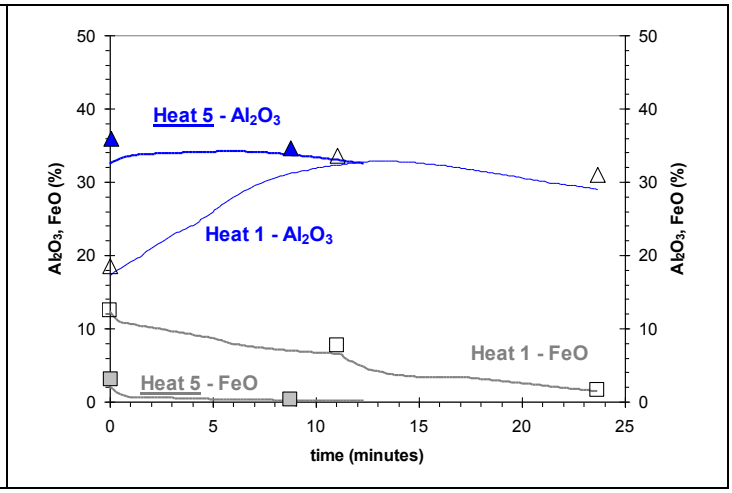

Figure 5b: Al_2O_3 and FeO concentrations of heat 1 and 5

Sulfur decreased at a slow constant rate during the treatment of heat 1 while it decreased at a fast exponential rate during the treatment of heat 5. The high FeO concentration during de-S and the high basicity of slag before the de-S caused the low de-S rate during the refining of heat 1 although it was stirred similarly well as heat 5. A high basicity of the slag decreases the activity coefficient of the FeO[10], slowing the reduction of the FeO by the aluminum. The aluminum decreased slower during heat 1 as compared to heat 5 although the FeO content of the slag was four times larger. The aluminum decreased at a fast, exponential rate during refining of heat 5, reducing the FeO that was produced on the slag/steel interface due to sulfur reduction. The addition of 750 lbs of bauxite to the slag of heat 1 during the first four minutes of de-S as compared to 250 lbs of bauxite addition before the Al-kill of heat 1 also hindered the de-S reactions at the slag/steel interface. The late bauxite addition raised the Al_2O_3 concentration of the slag, increasing the activity of Al_2O_3, which is a reaction product of de-S. In addition, the bauxite contained 26% hematite, adding to the FeO of the slag.

The FeO content of the slag during de-S influences the rate of de-S. Figure 6 illustrates the de-S reactions at the slag/steel interface together with the reactions that include the FeO from the slag. Iron oxides are supplied to the slag/steel interface by the reduction of sulfur[11], by the liquid FeO, by the air[12], and by sources that include bauxite, solid oxidized slags, refractory corrosion, and/or an oxidized scull from the LMF roof. The existing liquid FeO may originate from EAF carry-over slag, slag from the previous heat (estimated to be ½ ton), oxidized steel heel from the previous heat, and iron oxides produced during the cleaning of the porous plug and/or tap hole. These iron oxides need to be reduced by the deoxidant (in this case Al) for de-S to proceed.

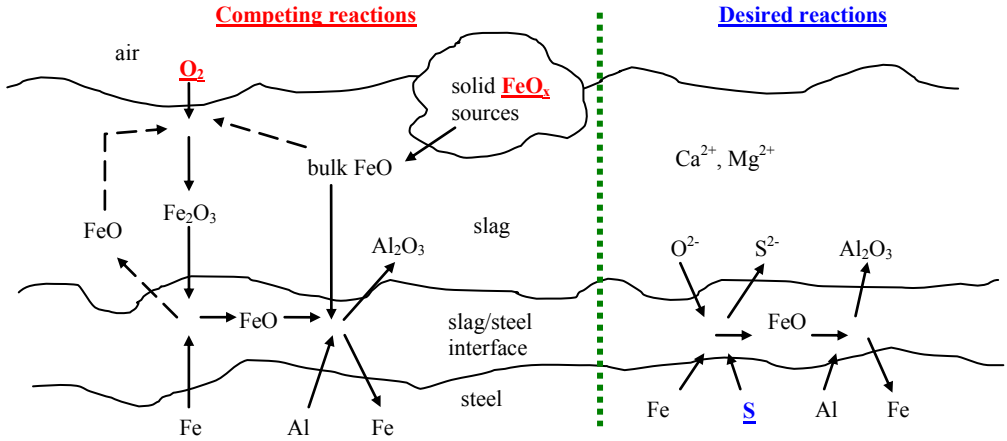

Figure 6: Illustration of desired de-S reactions and competing reactions within the slag and at the slag/steel interface

The reduction of sulfur also needs free oxygen anions or a basic slag, requiring the addition of lime after de-O. Lime additions not only increase the basicity of the slag but they also sustain de-S by maintaining or decreasing the concentration of Al_2O_3 or SiO_2. However, the increase of basicity causes a decrease of the activity coefficient of FeO[10]. The decrease of the activity coefficient of FeO during lime additions makes it increasingly more difficult to reduce the FeO after the de-S started. In addition, the ratio of Fe^{3+} and Fe^{2+} cations in the liquid slag increases with increasing basicity, sustaining the supply of oxygen from the air, through the slag, to the slag/steel interface[12]. Consequently, de-S rates are increased if the FeO is reduced before the basicity of the slag is raised with lime. This procedure was practiced during the treatment of heat 5 but not during the treatment of heat 1.

Apparent reaction order

High FeO concentration and basicity before de-S decreased the driving force ($C-C_{eq}$) more during the beginning of de-S than during the end of refining. This decrease resulted in a linear, slow reduction of the bulk sulfur concentration because the driving force remained effectively constant during de-S, implying a zero-order de-S reaction with respect to the driving force. However, Equation 1b assumes that de-S is a first-order reaction with respect to the driving force. The exponents that were calculated with Equation 1b were lower than the Metsim calculated mass transfer rate constants. The "apparent reaction order" (r) was defined as the quotient of the exponent from the line fit and the mass transfer rate constant (Equation 7). It ranged between 0.18 (heat 1) and 1.00 (heat 5).

Equation 7:

$$r = \frac{exponent\ from\ line\ fit}{k}$$

The bulk sulfur concentration decreased at a fast and exponential rate when the apparent reaction order was high or when the basicity and the FeO concentration were low before de-S started, indicating a relationship between the apparent reaction order and the basicity and FeO concentration. Equation 8a is the result of a line fit between the apparent reaction order of heats 1 to 12 (LMF 1), producing Al-killed steel, and ratio of the inverse exponential of the B-ratio (e^{-B}) and the %FeO as measured before de-S. Equation 8b shows the result of a similar line fit for heats 13 to 20 (LMF 2), producing Si-deoxidized steel and using spar. The inverse exponential of the B-ratio (e^{-B}) was used because it is proportional to the activity coefficient of FeO. This relationship was estimated from reference 10. The relationships of Equations 8a and 8b and the corresponding data are shown in Figure 7. The B-ratio, the concentration of FeO as measured before the start of de-S are listed with the apparent reaction order and mass transfer rate constants in Table 5 for all 20 heats.

Equation 8a:

$$r_{Al} = 0.2 + \frac{28e^{-B}}{\%FeO}$$

Equation 8b:

$$r_{Si/CaF_2} = 0.31 + \frac{2.6e^{-B}}{\%FeO}$$

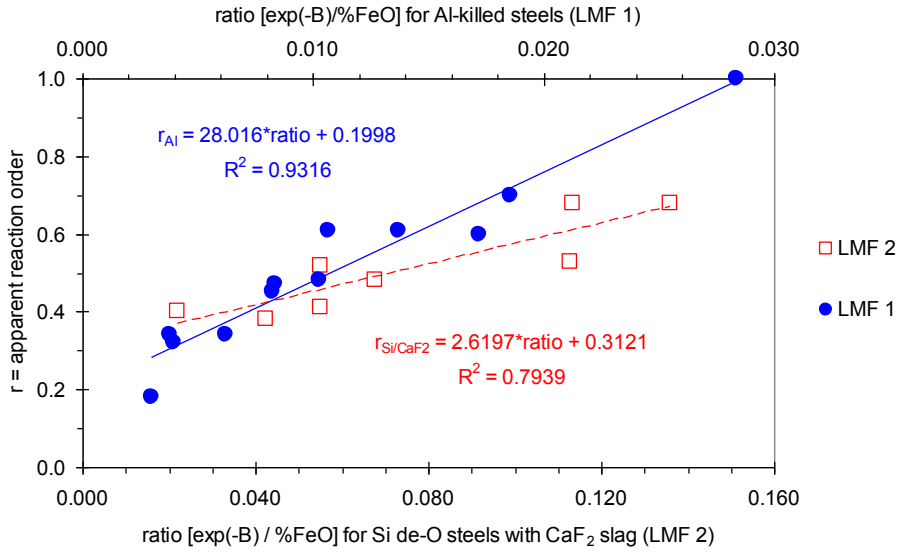

Figure 7: Relationships of Equations 8a (LMF 1) and 8b (LMF 2) are illustrated along with the corresponding data from Table 5

The basicity and the concentration of the FeO before de-S are lower for Si-deoxidized steel as compared to Al-killed steels for the same value of the apparent reaction order. The average B-ratio is 1.9 for Si-deoxidized steels (LMF 2) and 2.6 for Al-killed steels (LMF 1) because the slag of the heats from LMF 2 contained a maximum of 10% spar. Spar (CaF_2) is a strong base but it is not included in the B-ratio. The average FeO concentration before de-S is 3.1% in Si-deoxidized steels (LMF 2) and 9.0% for Al-killed steels (LMF 1) because the silicon is a weaker deoxidizer than the aluminum, requiring a lower FeO concentration before de-S can start. The lower affinity of silicon to oxygen causes the formation of SO_2 until the partial pressure of oxygen at the slag/steel interface and the FeO concentration of the slag are decreased. A peak of SO_2 in the off-gas is usually observed at the beginning of the ladle treatment at LMF 2[13].

The wide range of the exponents that were obtained from a line fit of the de-S data from Al-killed steels (LMF 1) in Figure 3 could be explained with the deoxidation strength of aluminum because the use of aluminum makes it possible to start the de-S at higher FeO concentrations as in Si-deoxidized steel if lime is added early. However, lime additions (beyond tap additions) before the FeO is reduced prolong the necessary time to achieve the final bulk sulfur concentration. The exponents from the line fit of de-S data from Si-deoxidized steels (LMF 2) in Figure 3 follow a straight line, indicating that a similar low FeO concentration at the beginning of de-S is necessary for all Si-deoxidized heats. However, a low basicity of the slag until the FeO is reduced improves de-S rates as well.

Table 5: B-ratios and %FeO after de-O but before de-S, apparent reaction order (r), mass transfer rate constant (k)

LMF 1													
Heat number		1	2	3	4	5	6	7	8	9	10	11	12
B ratio		3.3	2.3	2.5	2.5	2.4	2.9	2.5	2.9	2.3	3.1	2.5	2.4
% FeO		12.4	12.0	6.0	7.7	3.2	14.0	10.0	3.2	5.4	12.0	8.0	14.6
r		0.18	0.47	0.61	0.61	1.00	0.32	0.45	0.60	0.70	0.34	0.48	0.34
k	min^{-1}	0.19	0.18	0.18	0.20	0.20	0.17	0.17	0.18	0.20	0.20	0.16	0.21

LMF 2															
Heat number		13			14	15	16	17			18			19	20
B ratio		1.8			1.8	1.5	2.1	2.0			2.0			2.4	n/a
% FeO		3.0			3.9	10.2	0.9	1.2			2.0			0.8	
r		0.52	0.52	0.41	0.38	0.40	0.68	0.53	-	0.53	0.48	-	0.48	0.68	0.65
k	min^{-1}	0.05	0.05	0.11	0.12	0.08	0.06	0.10	0	0.06	0.12	0	0.07	0.10	0.08

Decarburization of the steel during argon purging

Heats 13 through 20 were argon purged during the first five to nine minutes of the treatment at LMF 2, causing a decrease of the carbon concentration that ranged between 0.005 %C (heat 18) and 0.012 %C (heat 13). The treatment of the steel during this time was argon stirring and arcing during a maximum of 64% of the purging time. The lime addition during de-C was 120 lbs during heats 14 and 16 and no lime for the other six heats. FeSi, SiMn and additional fluxes were added after de-C.

Figure 8 shows that the de-C rate was highest (0.0025 %C /min) when the FeO concentration increased by 5.0% during the argon purge (heat 13) and lowest (0.0006 %C /min) when the FeO concentration decreased by 2.0% (heat 18). The change of the FeO concentration was controlled by the duration of arcing so that the rate of de-C was actually a function ($R^2 = 0.85$) of the percentage of time that the heat was arced during purging. Long times of arcing reduced the de-C rate, independently of the argon flow rate.

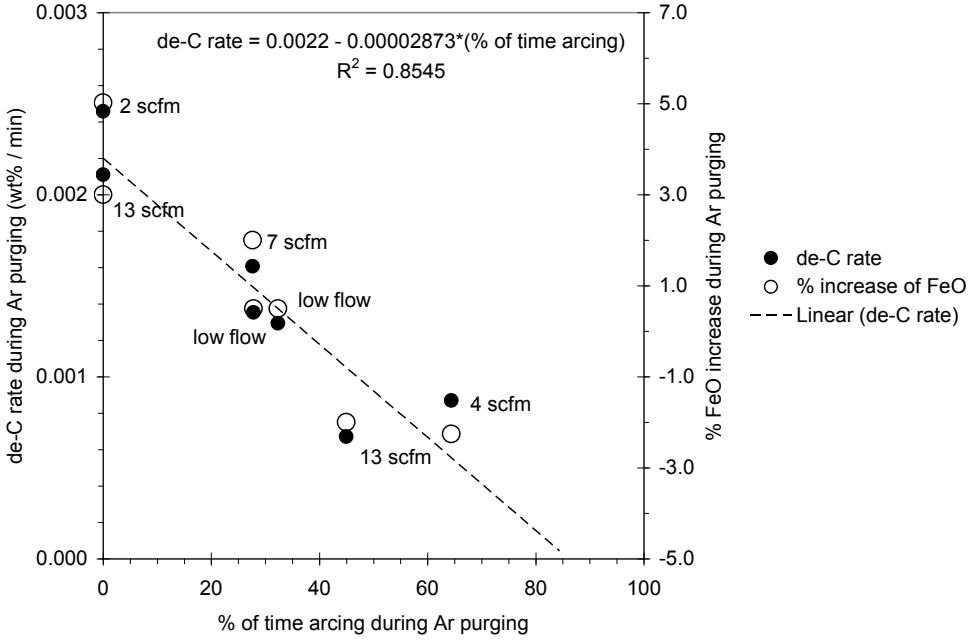

Figure 8: The de-C rate is described as a function of the change of FeO concentration and the duration of arcing during argon purging

The increase of the FeO concentration of the slag and the decrease of carbon concentration of the steel were caused by the transfer of oxygen from the air, through the slag, into the steel. The mechanism was illustrated in Figure 6. The arcing with carbon electrodes reduced the FeO in the slag and hindered the transfer of oxygen from the air into the slag, inhibiting a carbon boil below the slag. The carbon boil was sustained when arcing was stopped, indicating that solid sources of iron oxides (e.g. oxidized solid slag) were not the source of the FeO increase because solids would have preferable been melted during arcing.

Nitrogen increase and oxygen sources
The average nitrogen increase was 0.25 ppm per minute, independently of argon flow rate. The removal of the nitrogen by the rising argon was slightly lower as the absorption of nitrogen at the open eye, independently of the duration of arcing. However, the removal of nitrogen during the carbon boil of heats 13 through 20 was larger than the absorption of nitrogen through the open eye although the oxygen and sulfur concentrations were still high. The nitrogen remained constant or decreased by a maximum of 5 ppm (heat 17) during the carbon boil. The nitrogen concentration in the steel did not change when the argon was temporally turned off during the treatment of heats 17 and 18.

The air intake was adjusted during the simulation of each heat as dictated by the measured nitrogen. It was assumed that nitrogen is only absorbed by the steel but not the slag and that the steel absorbs nitrogen according to the thermodynamical equilibrium if air is in contact with the steel. The maximum air absorption through the open eye was 17.2 cubic feet of 2900ºF air per minute at an argon flow rate of 63 scfm. The absorption of oxygen through the open eye from this amount of air equals an equivalent of 7 lbs of Fe_2O_3 over a maximum stir period of 40 minutes, assuming that all the oxygen of this air is transferred to the steel. This amount of oxygen is significant less than the oxygen that was absorbed by the slag from the air or added to the slag by other sources.

The measured concentration changes of deoxidants (Al or Si), sulfur, vanadium, manganese, MnO, and FeO required the addition of 53 lbs (heat 5) to 540 lbs (heat 12) of Fe_2O_3 to the slag as an oxygen source during each simulation. At the average, 90 lbs of Fe_2O_3 were added during the simulation of each heat, independently of the FeO concentration in the slag. These 90 lbs have an approximate volume of three gallons and represent the iron oxide from sources that include solid slags, refractory corrosion, or miscellaneous sources such as an oxidized scull from the LMF roof. In addition, an average of 1.4 lbs of Fe_2O_3 had to be added per minute of refining time for each percent of FeO in the slag. In other words, the amount of oxygen that was transferred from the air through the slag to the slag/steel interface per minute by one percent of FeO was equal to the amount of oxygen from 140 cubic feet of 2900ºF air.

SUMMARY

The process simulation program Metsim and the thermodynamical program FactSage were used to model and simulate the ladle refining at two different LMF's, refining Al-killed and Si-deoxidized steels. The simulations could reproduce measured steel and slag concentrations during all times and for all heats. Twenty six mass transfer rate constants were determined during the simulations of twenty heats. The relationship between the mass transfer rate constant (k) and the argon flow rate, ladle geometry, ambient pressure, as well as steel temperature is best described with the specific steel transport rate (Equation 5c).

The reaction kinetics during ladle refining do not only depend on the bulk transport of the steel to the slag/steel interface (k) but also on the thermodynamical equilibrium at the slag/steel the interface. Desulfurization reactions are slow and nearly zero-order reactions with respect to the driving force ($C-C_{eq}$) if the FeO concentration of the slag is not reduced before the start of de-S and when the activity coefficient of FeO is low during the deoxidation reactions. Lime additions (beyond tap additions) before the FeO is reduced prolong the necessary time to achieve the final sulfur concentration because lime additions raise the basicity of the slag and therefore lower the activity coefficient of the FeO. Lime needs to be added to start and to sustain de-S. Lime additions raise the basicity of the slag and decrease or maintain the Al_2O_3 or SiO_2 concentrations.

The supply of iron oxides to the ladle before and during the refining needs to be minimized because iron oxides have to be reduced before de-S can proceed. More oxygen enters the steel from the air through the slag than during the open eye if the slag contains FeO. The transfer of oxygen from the air through slag to the slag/steel interface is large enough to sustain a carbon decrease of 0.0025 %C per minute. The average nitrogen increase during refining is 0.25 ppm N per minute.

ACKNOWLEDGEMENT

This material is based upon work supported by the U.S. Department of Energy under cooperative agreement number DE-FC36-03ID14279. Such support does not constitute an endorsement by DOE of the views expressed in the article.
The authors also appreciate the contributions from Nucor Steel Arkansas and Nucor-Yamato Steel. Special thanks go to late Joyce Crosskno as well as Robert Wyatt, Travis Barnes, Greg Mathis, Gary McQuillis, Hazel Scott, Dhiren Panda, Jim Swinford, and Gary Pennell from Nucor-Yamato Steel and Don Jackson, Sean Najafi, Billy Smith, Steve Segars, Heath Brown, Stephen Hickerson, Russel Talley, Lina Fritsche, Kent Patillo, Wilson Hubbard, Darrin Watson, Thomas Cash, P.K. Ghosh, Thomas Williams, Shannon Miller, and Bob McCracken from Nucor Steel Arkansas. Last but not least, we would also acknowledge the work from UMR students Jeremy Bryant and Cole Ely.

REFERENCES

1. Lachmund, H., Xie, Y., Buhles, T., Pluschkel, W. "Slag Emulsification during Liquid Steel Desulphurisation by Gas Injection into the Ladle" steel research, 2003, Vol. 74, No. 2, pp. 77-85
2. Grip, C.E., Jonsson, L. "Physical Behavior of slag in a 107-tonne ladle: production scale experiments and theoretical simulation" Scandinavian Journal of Metallurgy, 2003, Vol 32, No. 3, pp. 113-122
3. El-Kaddah, N., Szekely, J. "Mathematical model for desulphurization kinetics in argon-stirred ladles" Iron and Steelmaking , 1981, Vol. 8, No. 6, pp. 269 – 278
4. Mannering, T. e-mail from January 5th, 2005
5. Ghosh, A. "Secondary Steelmaking Principles and Applications" CRC Press, Boca Raton, London, New York, Washington DC, p. 203
6. Qu, Y. "Mass transfer coefficients in metallurgical reactors" Journal of University of Science and Technology Bejing, April 2003, Vol. 10, No. 2, pp. 1-9
7. Lehner, T. "Reactor models for powder injection" Scaninject (International Conference on Injection Metallurgy) , Luleå, Sweden, June 9-10, 1977, pp. 11:1-11:48
8. Aoki, J., Thomas, B.G., Peter, J., Peaslee, K.D. "Experimental and Theoretical Investigation of Mixing in a Bottom Gas-Stirred Ladle" AISTech 2004, Iron & Steel Technology Conference Proceedings, September 15-17, 2004, Vol. 1, pp. 1045-1056
9. Zlokarnik, M. "Homogenisieren von Flüssigkeiten durch aufsteigende Gasblasen" Chemie-Ing.-Techn., 1968, Vol. 40, No. 15, pp. 765-768
10. Turkdogan, E.T. "Fundamentals of Steelmaking" 1996, The University Press, Cambridge, UK, Fig. 5.22, p. 155
11. Robertson, D.G.C., Deo, B., Ohguchi, S. "Multicomponent mixed-transport-control theory for kinetics of coupled slag/metal and slag/metal/gas reactions: application to desulphurization of molten iron" Iron and Steelmaking, 1984, Vol. 11, No. 1, pp. 41-55
12. Turkdogan, E.T. "Fundamentals of Steelmaking" 1996, The University Press, Cambridge, UK, Sec. 5.6.4, p. 165
13. Panda, D. e-mail from January 21st, 2005